

Homes' law in holographic superconductor with linear- T resistivity

Hyun-Sik Jeong^{a,b} and Keun-Young Kim^c

^a*School of physics & CAS Center for Excellence in Topological Quantum Computation, University of Chinese Academy of Sciences, Zhongguancun east road 80, Beijing 100049, China*

^b*Kavli Institute for Theoretical Sciences, University of Chinese Academy of Sciences, Zhongguancun east road 80, Beijing 100049, China*

^c*School of Physics and Chemistry, Gwangju Institute of Science and Technology, 123 Cheomdan-gwagiro, Gwangju 61005, Korea*

E-mail: hyunsik@ucas.ac.cn, fortoe@gist.ac.kr

ABSTRACT: Homes' law, $\rho_s = C \sigma_{DC} T_c$, is a universal relation of superconductors between the superfluid density ρ_s at zero temperature, the critical temperature T_c and the electric DC conductivity σ_{DC} at T_c . Experimentally, Homes' law is observed in high T_c superconductors with linear- T resistivity in the normal phase, giving a material independent universal constant C . By using holographic models related to the Gubser-Rocha model, we investigate how Homes' law can be realized together with linear- T resistivity in the presence of momentum relaxation. We find that strong momentum relaxation plays an important role to exhibit Homes' law with linear- T resistivity.

Contents

1	Introduction	1
2	Superconductor based on the Gubser-Rocha model	3
2.1	Model	3
2.2	Linear- T resistivity in strange metal phase: a quick review	4
2.3	Superconducting phase and the coupling $B(\phi)$	6
2.3.1	UV completion of $B(\phi)$	7
2.3.2	Superconducting instability with T_c	8
3	Homes' law	11
3.1	Setup for numerics	11
3.2	Electric conductivity and superfluid density	12
3.3	Homes' law at strong momentum relaxation	16
3.4	The coupling τ dependence	18
4	Conclusions	19

1 Introduction

Holographic methods (gauge/gravity duality) have been providing novel and effective ways to study universal properties of strongly correlated systems. The representative examples would be the holographic lower bound of the ratio of shear viscosity to entropy density, linear- T resistivity and Hall angle of strange metals [1–6].

In this paper, using holography, we study another universal property of strongly coupled systems, which is observed in high T_c superconductors and some conventional superconductors: Homes' law [7, 8]. Homes' law is an empirical relation between the superfluid density at $T = 0$ ($\rho_s(T = 0)$), the phase transition temperature (T_c), and the electric DC conductivity in the normal phase close to T_c ($\sigma_{DC}(T_c)$):

$$\rho_s(T = 0) = C \sigma_{DC}(T_c) T_c, \quad (1.1)$$

where C is a material independent universal constant. For instance, $C \sim 4.4$ for ab-plane high T_c superconductors and clean BCS superconductors or $C \sim 8.1$ for c-axis high T_c superconductors and BCS superconductors in the dirty limit.

In order to study Homes' law in holography, first one may need to construct the holographic superconductor model. Using the complex scalar field, the holographic superconductor model was originally proposed by Hartnoll, Herzog, and Horowitz [9, 10] (the HHH model). Thereafter, there has been extensive development and extension of the HHH

model in [5, 6, 11, 12]. For the recent development of holographic superconductors, see also [13–18] and references therein.

Since the HHH model is a translational invariant theory, σ_{DC} is infinite so C in (1.1) is not well defined. Thus, in order to investigate Homes’ law, one may need to break the translational invariance to render σ_{DC} finite. In holography, there are several methods to incorporate momentum relaxation and yield a finite σ_{DC} . For instance, the bulk fields in gravity with the inhomogeneous boundary conditions [19], massive gravity models [20], Q-lattice models [21], the linear axion model [22], and the helical lattice model with a Bianchi VII₀ symmetry [23]. Using these models, holographic superconductors in the presence of the momentum relaxation have been investigated in [24–35].

In the aforementioned holographic superconductor models with momentum relaxation, Homes’ law has been studied only in several models [24, 32, 33].¹ For those models, there are parameters for the strength of momentum relaxation, which may specify material properties. Thus, in the holographic setup, Homes’ law means that C in (1.1) is constant independent of momentum relaxation parameters. In [24], using *the helical lattice model*, Homes’ law was studied with the amplitude and the pitch of the helix as momentum relaxation parameters. In [32], *the linear axion model* was studied for Homes’ law with the proportionality constant to spatial coordinate, k in (2.7), for the strength of momentum relaxation.² In [33], *the Q-lattice model* was used to study Homes’ law with the lattice amplitude/wavenumber for momentum relaxation parameter.

In all holographic studies so far, Homes’ law has not been well realized in that, in [24, 33], Homes’ law is satisfied only for some restricted parameter regime in which underlying physics has not been clearly understood yet or Homes’ law is not simply satisfied in [32]. Therefore, the fundamental understanding and the physical mechanism of Homes’ law is still lacking and it would be important to study Homes’ law with other holographic models.

In this paper, we study Homes’ law in the holographic superconductor model based on *the Gubser-Rocha model* [42] with the axion field to have momentum relaxation [35, 43–46].³ Our main motivation to choose this model is that it exhibits linear- T resistivity in its normal phase [35, 43, 44]. In particular, in [35], it was shown that the linear- T resistivity is robust above T_c in the *strong* momentum relaxation limit, which is similar to the experimental result for normal phases (strange metal phases) of high T_c superconductors. We will examine if Homes’ law can appear also in the strong momentum relaxation limit and also study its relation with the linear- T resistivity.

The property of linear- T resistivity is important for two reasons. First, it is another universal property in the normal phase of high T_c superconductors, so it is in fact a necessary property even before discussing Homes’ law. Second, it has been proposed that the Homes’ law can be explained by considering the Planckian dissipation [47], which is related with the linear- T resistivity. Therefore, the linear- T resistivity can be a key to understand

¹See [36] for an early attempt to study Homes’ law in holography without momentum relaxation. See also [34] for a modified version of Homes’ law with Weyl corrections.

²With the linear axion model, the normal phase has been studied in [29, 37–39], the superconducting phase in [28, 29], and the fermionic phase in [40]. See also [41] for the review/recent development of the holographic axion model.

³When we remove a dilaton field in the Gubser-Rocha model, it becomes the linear axion model in [32].

the physics of Homes' law. Because there has been no holographic model studying Homes' law together with linear- T resistivity⁴ our study is a necessary and important step to investigate Homes' law. Moreover, the Gubser-Rocha model with the axion field allows an analytic solution so that more tractable analysis is available for the normal phase. Note that most holographic studies in [24, 32, 33] do not allow analytic solution for normal phase so one needs to resort to numerical methods.

As one of the ingredient of our holographic superconductor model, inspired by [49, 50], we introduce the non-trivial coupling, $B(\phi)$, between the dilaton field ϕ and the complex scalar field Φ for condensate, and study the role of the coupling in Homes' law. In [49, 50], using the scaling property from $B(\phi)$, the superconducting instabilities have been investigated in which the translational invariance was not broken. Thus, our work might be considered as its generalization with momentum relaxation. Note that $B(\phi)$ was taken to be a mass term of Φ , $B(\phi) = M^2$, in the previous literature for Homes' law [24, 32, 33]. We find that Homes' law may not be realized with this trivial mass term.

This paper is organized as follows. In section 2, we introduce the holographic superconductor models based on the Gubser-Rocha model with the axion fields. In normal phase, we review how to obtain the linear- T resistivity analytically. For superconductor phase, we introduce the coupling term $B(\phi)$ and review its properties. We also study superconducting instability with T_c . In section 3, we numerically compute the optical conductivity and study the superfluid density. Using the linear- T resistivity in section 2 with the superfluid density in section 3, we study Homes' law. We also discuss the role of the coupling $B(\phi)$ for Homes' law. In section 4, we conclude.

2 Superconductor based on the Gubser-Rocha model

2.1 Model

We study a holographic superconductor model based on Einstein-Maxwell-Dilaton-Axion theory:

$$\begin{aligned} S &= S_1 + S_2 + S_3 = \int d^4x \sqrt{-g} (\mathcal{L}_1 + \mathcal{L}_2 + \mathcal{L}_3) , \\ \mathcal{L}_1 &= R - \frac{1}{2}(\partial\phi)^2 - \frac{1}{4}e^{\frac{\phi}{\sqrt{3}}} F^2 + 6 \cosh\left(\frac{\phi}{\sqrt{3}}\right) , \\ \mathcal{L}_2 &= -\frac{1}{2} \sum_{I=1}^2 (\partial\psi_I)^2 , \quad \mathcal{L}_3 = -|D\Phi|^2 - B(\phi)|\Phi|^2 , \end{aligned} \tag{2.1}$$

where we set units such that the AdS radius $L = 1$, and the gravitational constant $16\pi G = 1$. The action (2.1) consists of three actions. The first action S_1 is the Einstein-Maxwell-Dilaton theory, which is called 'Gubser-Rocha model' [42] composed of three fields: metric $g_{\mu\nu}$, a $U(1)$ gauge field A_μ with the field strength $F = dA$, and the scalar field ϕ so called 'dilaton'. The metric and gauge field are for a quantum field theory at finite temperature and density, while the dilaton field was originally introduced to make the vanishing entropy

⁴Note that other holographic studies for Homes' law [24, 32, 33] did not show the linear- T resistivity.

density (s) at zero temperature (T) as $s \sim T$ [42, 43]. The second action S_2 is added for the momentum relaxation: the ‘axion’ field ψ breaks the translational invariance so that the resistivity becomes finite [22, 35, 43–45].⁵ The third action S_3 is for the superconducting phase [9], which is composed of a complex scalar field Φ , the coupling $B(\phi)$, and the covariant derivative defined by $D_\mu := \nabla_\mu - iqA_\mu$.

The action (2.1) yields the equations of motion of matter fields

$$\nabla_\mu (e^{\frac{\phi}{\sqrt{3}}} F^{\mu\nu}) - iq\Phi^*(\partial^\nu - iqA^\nu)\Phi + iq\Phi(\partial^\nu + iqA^\nu)\Phi^* = 0, \quad (2.2)$$

$$\nabla^2\phi - \frac{1}{4\sqrt{3}}e^{\frac{\phi}{\sqrt{3}}}F^2 + 2\sqrt{3}\sinh\left(\frac{\phi}{\sqrt{3}}\right) - B'(\phi)|\Phi|^2 = 0, \quad (2.3)$$

$$\nabla^2\psi_I = 0, \quad (2.4)$$

$$D^2\Phi - B(\phi)\Phi = 0, \quad (2.5)$$

and the Einstein’s equation

$$\begin{aligned} R_{\mu\nu} - \frac{1}{2}g_{\mu\nu} \left[R - \frac{1}{4}e^{\frac{\phi}{\sqrt{3}}}F^2 - \frac{1}{2}(\partial\phi)^2 + 6\cosh\left(\frac{\phi}{\sqrt{3}}\right) - \frac{1}{2}\sum_{I=1}^2(\partial\psi_I)^2 - |D\Phi|^2 - B(\phi)|\Phi|^2 \right] \\ = \frac{1}{2}e^{\frac{\phi}{\sqrt{3}}}F_{\mu\delta}F_{\nu}{}^\delta + \frac{1}{2}\partial_\mu\phi\partial_\nu\phi + \frac{1}{2}\sum_{I=1}^2(\partial_\mu\psi_I\partial_\nu\psi_I) + \frac{1}{2}(D_\mu\Phi D_\nu^*\Phi^* + D_\nu\Phi D_\mu^*\Phi^*) . \end{aligned} \quad (2.6)$$

2.2 Linear- T resistivity in strange metal phase: a quick review

Let us first review the normal phase ($\Phi = 0$), $S = S_1 + S_2$, i.e., the Gubser-Rocha model with momentum relaxation. The purpose of this review is not only to organize this paper in a self-contained manner, but also collect useful results, linear- T resistivity, to study our main objective, Homes’ law, in section 3. We refer to [35] for more detailed explanation of the normal phase.

In normal phase ($\Phi = 0$), the analytic solution is available [35, 44, 45, 50]:

$$\begin{aligned} ds^2 &= -f(r)dt^2 + \frac{1}{f(r)}dr^2 + h(r)(dx^2 + dy^2), \\ f &= r^{1/2}(r+Q)^{3/2} \left(1 - \frac{k^2}{2(r+Q)^2} - \frac{(r_h+Q)^3}{(r+Q)^3} \left(1 - \frac{k^2}{2(r_h+Q)^2} \right) \right), \\ h &= r^{1/2}(r+Q)^{3/2}, \\ A_t &= \sqrt{3Q(r_h+Q) \left(1 - \frac{k^2}{2(r_h+Q)^2} \right)} \left(1 - \frac{r_h+Q}{r+Q} \right), \quad \phi = \frac{\sqrt{3}}{2} \ln(1+Q/r), \\ \psi_1 &= kx, \quad \psi_2 = ky, \end{aligned} \quad (2.7)$$

where r_h denotes the horizon radius, k controls a strength of the momentum relaxation, and Q is a parameter which can be expressed with physical parameters: temperature

⁵The axion-type model is related to the Stückelburg formulation of a massive gravity theory [20, 51–53].

(T), chemical potential (μ) or momentum relaxation parameter (k). The temperature and chemical potential reads

$$T = \frac{f'(r)}{4\pi} \Big|_{r_h} = r_h \frac{6(1 + \tilde{Q})^2 - \tilde{k}^2}{8\pi(1 + \tilde{Q})^{3/2}} = r_h \tilde{T}, \quad (2.8)$$

$$\mu = A_t(\infty) = r_h \sqrt{3\tilde{Q}(1 + \tilde{Q}) \left(1 - \frac{\tilde{k}^2}{2(1 + \tilde{Q})^2}\right)} = r_h \tilde{\mu}, \quad (2.9)$$

where

$$\tilde{Q} := \frac{Q}{r_h}, \quad \tilde{k} := \frac{k}{r_h}, \quad \tilde{T} := \frac{T}{r_h}, \quad \tilde{\mu} := \frac{\mu}{r_h}. \quad (2.10)$$

Now one can obtain the dimensionless physical quantities at finite density, T/μ and k/μ , as

$$\bar{T} := \frac{T}{\mu} = \frac{\tilde{T}}{\tilde{\mu}} = \frac{6(1 + \tilde{Q})^2 - \tilde{k}^2}{4\sqrt{6\pi} \sqrt{\tilde{Q}(1 + \tilde{Q})^2(2(1 + \tilde{Q})^2 - \tilde{k}^2)}}, \quad (2.11)$$

$$\bar{k} := \frac{k}{\mu} = \frac{\tilde{k}}{\tilde{\mu}} = \sqrt{\frac{2(1 + \tilde{Q})\tilde{k}^2}{3\tilde{Q}(2(1 + \tilde{Q})^2 - \tilde{k}^2)}}, \quad (2.12)$$

where we used (2.8)-(2.10).

The linear- T resistivity: The electric DC conductivity at $\Phi = 0$ can be obtained [38, 39, 52, 54] as

$$\sigma_{DC} := e^{\frac{\phi}{\sqrt{3}}} + \frac{A_t^2 h(r) e^{\frac{2\phi}{\sqrt{3}}}}{k^2} \Big|_{r \rightarrow r_h} = \sqrt{1 + \tilde{Q}} + \frac{\sqrt{1 + \tilde{Q}}}{\tilde{k}^2}. \quad (2.13)$$

Using (2.11)-(2.12), one can express \tilde{Q} as a function of \bar{T} and \bar{k} analytically, i.e. $\tilde{Q}(\bar{T}, \bar{k})$, this implies that the electric DC conductivity (2.13) can also be expressed in terms of \bar{T} and \bar{k} as $\sigma_{DC}(\bar{T}, \bar{k})$.

With the analytic expression of $\tilde{Q}(\bar{T}, \bar{k})$, one can find that the Gubser-Rocha model can exhibit linear- T resistivity, the resistivity ($\rho = 1/\sigma_{DC}$) is linear in temperature, for two cases⁶

$$\sigma_{DC} \sim \frac{\sqrt{3} \left(1 + \bar{k}^2\right)^2}{2\pi \bar{k}^2 \sqrt{4 + 6\bar{k}^2}} \frac{1}{\bar{T}}, \quad (\bar{T} \ll 1 \text{ for given } \bar{k}), \quad (2.14)$$

$$\sigma_{DC} \sim \frac{\bar{k}}{2\sqrt{2}\pi \bar{T}}, \quad (\bar{k} \gg 1 \text{ for given } \bar{T}), \quad (2.15)$$

⁶For more details, see [35].

where $\tilde{Q}(\bar{T}, \bar{k})$ has the asymptotic form as

$$\tilde{Q} \sim \frac{3(1 + \bar{k}^2)^2}{8\pi^2(2 + 3\bar{k}^2)\bar{T}^2}, \quad (\bar{T} \ll 1 \text{ for given } \bar{k}), \quad (2.16)$$

$$\tilde{Q} \sim \frac{\bar{k}^2}{8\pi^2\bar{T}^2}, \quad (\bar{k} \gg 1 \text{ for given } \bar{T}). \quad (2.17)$$

The former case ($\bar{T} \ll 1$), (2.14), is related to the result in [43] and this linear- T resistivity is due to the fact that the Gubser-Rocha model has the Conformal to $\text{AdS}_2 \times R^2$ IR geometry [55].⁷ The other case ($\bar{k} \gg 1$), (2.15), will be one of important ingredients of our main results for Homes' law in section 3.⁸

2.3 Superconducting phase and the coupling $B(\phi)$

Let us study the superconducting phase based on the Gubser-Rocha model, $S = S_1 + S_2 + S_3$ (2.1), which will also be used for Homes' law in section 3. Note that in order for the description of holographic superconductors, first we need to specify the form of the coupling $B(\phi)$. In this section 2.3, we first review how to introduce the coupling (2.25) chosen in this paper and study the superconducting instability with the critical temperature T_c .

Although we will examine Homes' law with the fully back-reacted background geometry in section 3, it would be instructive to treat a complex scalar field Φ as a perturbation field on top of the background geometry of Gubser-Rocha model (2.7).

There are three main reasons why we perform the perturbative (i.e., without back-reaction) analysis here. First, we can investigate the properties of the coupling $B(\phi)$ with the analytic IR scaling geometry. Moreover, one may also try to obtain the analytic instability condition. Second, we may use the perturbative analysis as a guide for the study of Homes' law in next section, i.e., we will study T_c , one of the main ingredients for Homes' law, in the simple (i.e., no back-reaction) setup and show that T_c from the perturbative analysis is consistent with T_c in the presence of the back-reaction. Third, our perturbative analysis for T_c will be an extension to the previous work [50] where the translational symmetry was not broken ($k/\mu = 0$).

Note that the analysis for T_c would be important not only for Homes' law, but also to find the condition for high T_c superconductors having linear- T resistivity. As we will show, the trivial coupling, $B(\phi) = M^2$, would not be enough to have the superconducting phases at strong momentum relaxation limit, which is connected to the normal phase showing linear- T resistivity (2.15).

⁷In the semi-locally critical limit where the dynamical exponent $z \rightarrow \infty$ and a hyperscaling violating exponent $\theta \rightarrow -\infty$ with the fixed $\theta/z = -\eta$, the Einstein-Maxwell-Dilaton-Axion theory has the Conformal to $\text{AdS}_2 \times R^2$ IR geometry with the parameter η and the resistivity behaves as $\rho \sim T^\eta$. The linear- T resistivity appears in Gubser-Rocha model because $\eta = 1$ for Gubser-Rocha model.

⁸Note that, as pointed it out in [35, 56], (2.14) may not guarantee that the linear- T resistivity is robust up to high temperature. Thus, phenomenologically (2.15) would be a more relevant condition to show the linear- T resistivity above T_c , which is similar to experiments and checked in holography [35].

2.3.1 UV completion of $B(\phi)$

Using the scaling properties in the IR region, one minimal way to choose the coupling $B(\phi)$ was introduced in [50]. Here we not only review the method in [50], but also extend the analysis in [50] to the case at finite k/μ .

The extremal IR geometry: In order to investigate the IR scaling properties, we first need to have the extremal IR geometry which can be obtained from (2.7) in $T \rightarrow 0$ limit. From (2.11), one can find the condition for $T = 0$ as $r_h/Q \rightarrow 0$ (or $\tilde{Q} \rightarrow \infty$). Note that there is another mathematical possibility to obtain $T = 0$ from the relation between \tilde{Q} and \tilde{k} such that $6(1 + \tilde{Q})^2 - \tilde{k}^2 = 0$. However, this another condition can be ruled out for the physical reason: it gives the imaginary chemical potential (2.9) and momentum relaxation (2.12).⁹

Then, using the condition $r_h/Q \rightarrow 0$ with the following coordinate transformation¹⁰ in (2.7)

$$\rho = \sqrt{\frac{Q}{3r}}, \quad t' = \sqrt{1 - \frac{k^2}{6Q^2}} t, \quad (2.18)$$

one can express the extremal IR geometry as

$$\begin{aligned} ds^2 &= \frac{Q^2}{\sqrt{3}} \frac{1}{\rho} \left[-\frac{dt'^2}{\rho^2} + \frac{8}{6Q^2 - k^2} \frac{d\rho^2}{\rho^2} + dx^2 + dy^2 \right], \\ A_{t'} &= \sqrt{\frac{2Q^2 - k^2}{6Q^2 - k^2}} \frac{Q}{\rho}, \quad \phi = \sqrt{3} \ln(\sqrt{3}\rho), \end{aligned} \quad (2.19)$$

where the IR is located at $\rho \rightarrow \infty$. Note that (2.19) corresponds to Conformal to $\text{AdS}_2 \times R^2$ geometry and it is consistent with the one in [50] at $k = 0$.

The coupling $B(\phi)$ in IR: The complex scalar field Lagrangian in (2.1), \mathcal{L}_3 , can be written as follows.

$$-\mathcal{L}_3 = (\partial\Phi)^2 + [q^2 A^2 + B(\phi)] \Phi^2, \quad (2.20)$$

where Φ can be taken to be real, since the radial component of the Maxwell equations implies the phase of Φ is constant. Note that the last two terms in (2.20) correspond to the effective mass term of Φ with the effective mass $m_{\text{eff}}^2 := q^2 A^2 + B(\phi)$.

Plugging the following scaling ansatz (2.21) into (2.20), we can study the scaling property of Φ with the IR geometry (2.19)

$$\Phi = \Phi_0 \rho^{\Delta_\Phi}, \quad B(\phi) := B_{\text{IR}}(\phi) = B_0 \rho^{\Delta_B}, \quad (2.21)$$

⁹Note also that \tilde{Q} should be positive to be thermodynamically stable [45].

¹⁰There would be other coordinate transformation to express Conformal to $\text{AdS}_2 \times R^2$ geometry. For the comparison with the previous literature [50], we have used (2.18).

and one can find that the kinetic term and the effective mass term behave as follows

$$(\partial\Phi)^2 \sim \rho^{2\Delta_\Phi+1}, \quad q^2 A^2 \Phi^2 \sim \rho^{2\Delta_\Phi-1}, \quad B_{\text{IR}}(\phi) \Phi^2 \sim \rho^{2\Delta_\Phi+\Delta_B}. \quad (2.22)$$

In general, one can notice that the gauge field contribution to the effective mass, $q^2 A^2 \Phi^2$ term, scales differently with the kinetic term, $(\partial\Phi)^2$. However, the contribution from the coupling $B(\phi)$, $B_{\text{IR}}(\phi) \Phi^2$, can scale in the same way as the kinetic term if

$$\text{Scaling case :} \quad \Delta_B = 1 \quad \Leftrightarrow \quad B_{\text{IR}}(\phi) = B_0 \rho \sim e^{\frac{\phi}{\sqrt{3}}}, \quad (2.23)$$

where a dilaton solution in (2.19) is used in the proportionality. This (2.23) is called “the scaling case” [50].

One can generalize (2.23) for the generic scaling IR behavior of $B(\phi)$ with the one parameter τ as

$$B_{\text{IR}}(\phi) = B_0 e^{\tau\phi}, \quad (2.24)$$

where $\tau = 1/\sqrt{3}$ corresponds to (2.23).

The UV-completed coupling $B(\phi)$: In principle, there would be many possibilities to choose the UV-completed coupling, $B(\phi)$, satisfying (2.24) in IR. In this paper, for concreteness in our discussion and numerics, we choose one minimal way studied in [50]:

$$B(\phi) = M^2 \cosh(\tau\phi), \quad (2.25)$$

where it has two parameters (M, τ) . Note that the coupling (2.25) is the same form of the dilaton potential in (2.1): $\cosh(\phi/\sqrt{3})$. In UV region ($r \rightarrow \infty$) (or $\phi \rightarrow 0$), the coupling (2.25) is expanded as

$$B_{\text{UV}}(\phi) \sim M^2 \left(1 + \frac{\tau^2}{2} \phi^2 + \dots \right), \quad (2.26)$$

and in IR region ($r \rightarrow 0$) (or $\phi \rightarrow \infty$) we have

$$B_{\text{IR}}(\phi) \sim \frac{M^2}{2} e^{\tau\phi}, \quad (2.27)$$

where B_0 in (2.24) is $M^2/2$. For concreteness in our numerics, we fix $M^2 = -2$ and $q = 6$ in this paper. We also make some further comments on M^2 at the end of this section. Note that we choose the same value for the charge of Φ , q , which was used in previous studies of Homes’ law [24, 32, 33] for an easy comparison.

2.3.2 Superconducting instability with T_c

Now we investigate the critical temperature T_c with (2.25), which might be important not only for Homes’ law, but also for the study of high T_c superconductors. We will determine

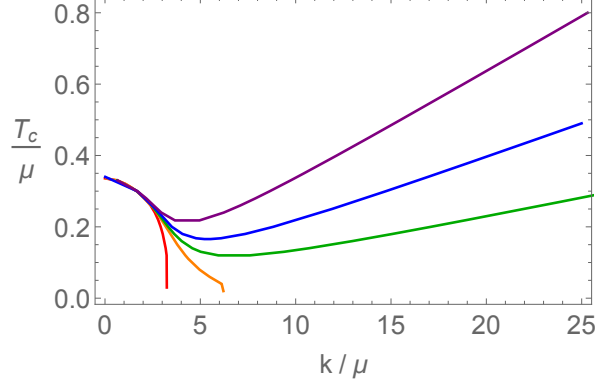


Figure 1. T_c vs k/μ with $\tau \in [0, \frac{1}{\sqrt{3}} \frac{12}{10}]$ (red-purple).

T_c by solving the complex scalar field equation of motion (2.5):

$$\Phi''(r) + \left(\frac{f'}{f} + \frac{h'}{h} \right) \Phi'(r) - \frac{1}{f} \left(B(\phi) - \frac{q^2 A_t^2}{f} \right) \Phi(r) = 0, \quad (2.28)$$

where we can use $f(r)$, $h(r)$, and $A_t(r)$ from (2.7) in the absence of the back-reaction.

In order to solve the equation of motion (2.28), we impose two boundary conditions. The first condition is from the horizon, r_h , with the regularity condition in which $\Phi'(r_h)$ will be determined by $\Phi(r_h)$. The second boundary condition comes from the AdS boundary, $r \rightarrow \infty$. Φ behaves near the AdS boundary as

$$\Phi(r) = \frac{\Phi^{(-)}}{r^{\Delta_-}} + \frac{\Phi^{(+)}}{r^{\Delta_+}} + \dots, \quad \Delta_{\pm} = \frac{3 \pm \sqrt{4M^2 + 9}}{2}. \quad (2.29)$$

By the holographic dictionary, the fast falloff of the field $\Phi^{(-)}$ is interpreted as the source and the slow falloff $\Phi^{(+)}$ corresponds to the condensate. As a boundary condition for superconductors, we set the source term, $\Phi^{(-)}$, to be zero to describe a spontaneous symmetry breaking. Thus, when $\Phi^{(+)}$ is finite the state will be a superconducting phase, while if $\Phi^{(+)} = 0$ (or $\Phi = 0$) the state corresponds to a normal phase.

The critical temperature T_c vs k/μ : Solving equation of motion (2.28) with the boundary conditions above, one can find T_c at which the condensate $\Phi^{(+)}$ starts to be finite.

In Fig. 1, we display the plot for T_c in terms of k/μ with various τ . In $k/\mu \ll 1$ region, one cannot find the τ effect on T_c , i.e., T_c is independent on τ in the coherent regime ($k/\mu \rightarrow 0$). This would be consistent with the result at $k/\mu = 0$ in [50].¹¹

However, as k/μ is increased, we find two main features related to τ . First, there would be a critical τ , τ_c , to study superconducting phases at $k/\mu \gg 1$ limit. For instance, if $\tau = \frac{1}{\sqrt{3}} \frac{8}{10}$ (orange) in Fig. 1, superconducting phases cannot be obtained in $k/\mu > 6$

¹¹Depending on the parameter regime in (q, M^2) , there would be a minimal charge q below which the superconducting instability with T_c does not exist [50]. Similar parameter regime may also appear in the presence of momentum relaxation, we leave it as future work.

regime. Therefore, in order to study superconductors in the strong momentum relaxation limit ($k/\mu \rightarrow \infty$), we need to consider $\tau > \tau_c$. In this paper, we take $\tau_c = \frac{1}{\sqrt{3}} \frac{8}{10}$ for simplicity: in Fig. 1, one may try to find a more exact value for τ_c between the orange one ($\tau_c = \frac{1}{\sqrt{3}} \frac{8}{10}$) and the green one ($\tau_c = \frac{1}{\sqrt{3}} \frac{9}{10}$).

Second, at given k/μ , τ enhances T_c (e.g., from green to purple). This indicates that the superconducting instability can be triggered more easily at higher coupling τ . Thus, a larger τ might be useful to investigate the superconducting phase at higher temperature, i.e., high T_c superconductors.

High T_c superconductor and linear- T resistivity: In summary, we find that the coupling τ , $\tau > \tau_c$, would be important not only for superconducting phases at strong momentum relaxation region, but also for high T_c superconductors.

Based on this result, we may argue that, in order to describe high T_c superconductors having linear- T resistivity (2.15) near T_c (i.e., the region where the normal phase still can be useful), we may need the following conditions:

$$\text{i) } \tau > \tau_c; \quad \text{ii) } k/\mu \gg 1. \quad (2.30)$$

This would imply that the trivial coupling term $B(\phi) = M^2$ ($\tau = 0$ case) used in most of the previous literature may not capture a complete feature of the superconducting phases at strong momentum relaxation limit. In the following section 3, we will study if the condition (2.30) can also be related to Homes' law.

Instability condition for M^2 : We finish this section with the instability condition for M^2 with the complex scalar field equation of motion. Here we consider the scaling case ($\tau = \frac{1}{\sqrt{3}}$) because one can obtain a simple analytic instability condition with it.¹²

At $\tau = \frac{1}{\sqrt{3}}$, the complex scalar field equation of motion in the IR geometry (2.19) can be expressed as

$$\Phi''(\rho) - \frac{1}{\rho} \Phi'(\rho) + \frac{4Q^2 (M^2(k^2 - 6Q^2)\rho^2 - 2q^2(k^2 - 2Q^2))}{(k^2 - 6Q^2)^2 \rho^4} \Phi(\rho) = 0, \quad (2.31)$$

and this equation can be solved analytically by the combination of Bessel functions J_ν :

$$\Phi(\rho) = c_1 \rho \Gamma(1-\nu) J_{-\nu} \left(\sqrt{\frac{8q^2 Q^2 (k^2 - 2Q^2)}{(k^2 - 6Q^2)^2}} \frac{1}{\rho} \right) + c_2 \rho \Gamma(1+\nu) J_\nu \left(\sqrt{\frac{8q^2 Q^2 (k^2 - 2Q^2)}{(k^2 - 6Q^2)^2}} \frac{1}{\rho} \right), \quad (2.32)$$

where the index ν is

$$\nu = \sqrt{\frac{k^2 - (6 + 4M^2)Q^2}{k^2 - 6Q^2}}. \quad (2.33)$$

¹²The same thing happens even at $k/\mu = 0$ in [50]. We cannot find the analog of the generalized BF bound unless $\tau = \frac{1}{\sqrt{3}}$. So, identifying the analytic expression for the onset of the phase transition for non-scaling case is still challenging.

Then, the instability appears when the index ν of Bessel function becomes imaginary. Note that, unlike the case of $k = 0$ in [50], there are two ways to make the imaginary ν depending on the sign of the numerator (or denominator) in ν : i) the positive numerator with the negative denominator; ii) the negative numerator with the positive denominator. Each case produces the following instability condition for M^2

$$M^2 < \frac{k^2 - 6Q^2}{4Q^2} < 0 \quad \text{or} \quad M^2 > \frac{k^2 - 6Q^2}{4Q^2} > 0. \quad (2.34)$$

Note that only the first condition in (2.34) is consistent at $k = 0$. Thus, from the perspective of continuity encompassing the $k = 0$ case, the first condition in (2.34) might be the proper instability condition.

3 Homes' law

In this section, considering the coupling (2.25), we study Homes' law with the fully back-reacted geometry.

3.1 Setup for numerics

We consider the following ansatz to obtain the fully back-reacted background solutions

$$\begin{aligned} ds^2 &= \frac{1}{\tilde{z}^2} \left[-(1 - \tilde{z})U(\tilde{z})d\tilde{t}^2 + \frac{d\tilde{z}^2}{(1 - \tilde{z})U(\tilde{z})} + V(\tilde{z})d\tilde{x}^2 + V(\tilde{z})d\tilde{y}^2 \right], \\ A &= (1 - \tilde{z})a(\tilde{z})d\tilde{t}, \quad \phi = \frac{\sqrt{3}}{2} \log[1 + \varphi(\tilde{z})], \quad \Phi = \tilde{z}^{\Delta_-} \eta(\tilde{z}), \\ \psi_1 &= \tilde{k} \tilde{x}, \quad \psi_2 = \tilde{k} \tilde{y}, \end{aligned} \quad (3.1)$$

where

$$\tilde{z} := \frac{z}{z_h}, \quad \tilde{t} := \frac{t}{z_h}, \quad \tilde{x} := \frac{x}{z_h}, \quad \tilde{y} := \frac{y}{z_h}, \quad \tilde{k} := k z_h. \quad (3.2)$$

Here U, V, a, φ and η are functions of the holographic direction \tilde{z} . In this coordinate, the AdS boundary is located at $\tilde{z} = 0$ and the horizon is at $\tilde{z} = 1$. Note that the coordinate (3.1) is related to (2.7) with $z = 1/r$ and the form of ansatz (3.1) is chosen for the convenience of numerical analysis for superconducting phase.

With the ansatz (3.1), one can identify the Hawking temperature T and the chemical potential μ as

$$T = \frac{g'_{tt}(\tilde{z})}{4\pi\sqrt{g_{tt}g_{\tilde{z}\tilde{z}}}} \Big|_{\tilde{z}=1} = \frac{U(1)}{4\pi}, \quad \mu = A_t(0) = a(0), \quad (3.3)$$

and the condensate $\Phi^{(+)}$ in (2.29) can be read off from η in (3.1) near the AdS boundary as

$$\Phi = \Phi^{(-)} \tilde{z}^{\Delta_-} + \Phi^{(+)} \tilde{z}^{\Delta_+} + \dots \Leftrightarrow \eta = \Phi^{(-)} + \Phi^{(+)} \tilde{z}^{\Delta_+ - \Delta_-} + \dots, \quad (3.4)$$

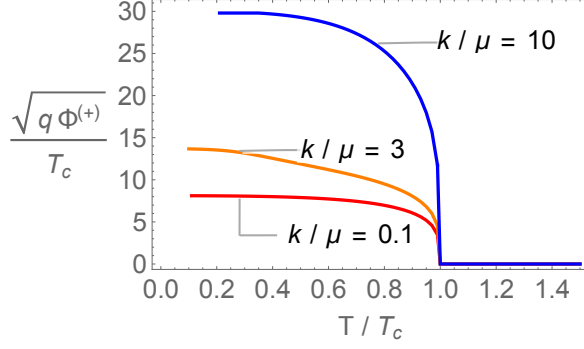


Figure 2. Condensation vs temperature at $\tau = 1/\sqrt{3}$ where T_c is the critical temperature.

where Δ_{\pm} is defined in (2.29).¹³

In order for the superconducting phases, we set the source $\Phi^{(-)} = 0$, i.e., $\eta(0) = 0$ and need to find the state with the finite condensate $\Phi^{(+)} \neq 0$. One can find such a state by solving the equations (2.2)-(2.6) numerically with the ansatz (3.1). The typical condensate is plotted in Fig. 2: the condensate tends to be enhanced with increasing k/μ and this seems to be a generic feature of holographic superconductors in the presence of the momentum relaxation.

In what follows, in section 3.2, we focus on the scaling case $\tau = 1/\sqrt{3} > \tau_c$ and study the electric optical conductivity $\sigma(\omega)$ and the superfluid density ρ_s . Then, using the results in section 3.2, we investigate Homes' law in section 3.3. In section 3.4, we discuss the τ effect on Homes' law.

3.2 Electric conductivity and superfluid density

Let us study the electric optical conductivity of the holographic model (2.1). From here on, we use the scaled variables (3.2) without tilde for simplicity.

Holographic electric optical conductivity: In order to compute the electric optical conductivity, we need to consider the following fluctuations:

$$\delta g_{tx} = h_{tx}(z) e^{-i\omega t}, \quad \delta A_x = a_x(z) e^{-i\omega t}, \quad \delta \psi_x = \xi_x(z) e^{-i\omega t}, \quad (3.5)$$

where the fluctuations behave near the AdS boundary as

$$\begin{aligned} h_{tx}(z) &= \frac{h_{tx}^{(S)}}{z^2} + h_{tx}^{(R)} + \dots, \\ a_x(z) &= a_x^{(S)} + a_x^{(R)} z + \dots, \\ \xi_x(z) &= \xi_x^{(S)} + \xi_x^{(R)} z + \dots, \end{aligned} \quad (3.6)$$

here the leading coefficients $(h_{tx}^{(S)}, a_x^{(S)}, \xi_x^{(S)})$ correspond to the sources, and the subleading terms $(h_{tx}^{(R)}, a_x^{(R)}, \xi_x^{(R)})$ would be interpreted as the response by the holographic dictionary.

¹³For $M^2 = -2$, $(\Delta_-, \Delta_+) = (1, 2)$.

The electric optical conductivity can be obtained by the Kubo formula in terms of the boundary coefficients in (3.6):

$$\sigma(\omega) = \frac{1}{i\omega} G_{j^x j^x}^R(\omega) = \frac{a_x^{(R)}}{i\omega a_x^{(S)}}, \quad (3.7)$$

where $G_{j^x j^x}^R$ is the current-current retarded Green's function. The second equality in (3.7) holds when $a_x^{(S)}$ is the only non-zero source.

In order to make the source-vanishing boundary condition except $a_x^{(S)}$, one may use the diffeomorphisms and gauge-transformations [21, 38]. With a constant residual gauge parameter ζ fixing $\delta g_{rx} = 0$ [38], it can be shown that the fluctuations in (3.5) except δA_x can be expanded near the AdS boundary as¹⁴

$$z^2 \delta g_{tx} \sim (h_{tx}^{(S)} - i\omega\zeta)e^{-i\omega t} = 0, \quad \delta\psi_x \sim (\xi_x^{(S)} + k\zeta)e^{-i\omega t} = 0, \quad (3.8)$$

where the equalities correspond to the source-vanishing boundary condition except $a_x^{(S)}$. Plugging one of the equations in (3.8) into the other, (3.8) produces a single condition

$$\xi_x^{(S)} - \frac{ik}{\omega} h_{tx}^{(S)} = 0. \quad (3.9)$$

Therefore, one can use (3.7) to study the electric optical conductivity by solving the equation of motion of the fluctuations with the boundary condition (3.9).

Electric optical conductivity in strange metal/superconductor transition: Using the method above, we make the plot of the optical conductivity in Fig. 3.¹⁵ The color of curves denotes a temperature ratio T/T_c : the dashed black is for the normal metal phase ($T > T_c$), the red line is for the critical temperature ($T = T_c$), and other colors (from orange to blue) correspond to the superconducting phase ($T < T_c$).

For $T \geq T_c$, one can see that the DC conductivity, $\sigma(\omega = 0)$, is finite due to the momentum relaxation¹⁶, while the superconducting phase ($T < T_c$) produces $1/\omega$ pole in $\text{Im}[\sigma]$ giving the infinite DC conductivity. By the Kramers-Kronig relation, $1/\omega$ pole in $\text{Im}[\sigma]$ implies that $\text{Re}[\sigma]$ has a delta function at $\omega = 0$: this is one of hallmarks of holographic superconductor.

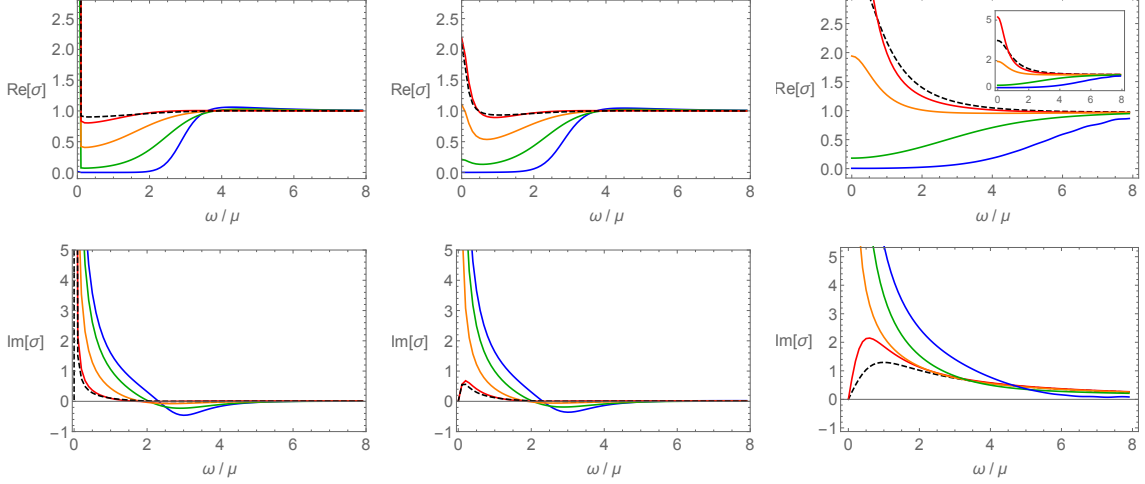
Let us make some further comments on the electric conductivity of our model (2.1). In holography, there are two simple gravity models to study the electric conductivity of the normal phase in the presence of the momentum relaxation: i) the linear axion model [22]¹⁷; ii) the Gubser-Rocha model with the axion field (2.1).

¹⁴For more detailed analysis and discussion about the diffeomorphism and gauge-transformations, see [21, 32, 38].

¹⁵We also checked that our numerical code produces the consistent result in [57]: the optical conductivity of the Gubser-Rocha model at $k/\mu = 0$.

¹⁶We checked that $\sigma(\omega = 0)$ is consistent with the analytic result in (2.13). For instance, see Fig. 4(b).

¹⁷Recall that the linear axion model is (2.1) without a dilaton field ϕ .



(a) $k/\mu = 0.1$, $T/T_c = 1.5, 1, 0.93$, (b) $k/\mu = 1$, $T/T_c = 1.5, 1, 0.93$, (c) $k/\mu = 10$, $T/T_c = 1.5, 1, 0.97, 0.75, 0.21$ (dashed, red, orange, 0.75, 0.21 (dashed, red, orange, green, blue) green, blue) (dashed, red, orange, green, blue)

Figure 3. Electric conductivity with various $k/\mu = 0.1, 1$ and 10 . The first row displays $\text{Re}[\sigma(\omega)]$, while $\text{Im}[\sigma(\omega)]$ is plotted in the second row ($\tau = 1/\sqrt{3}$).

In [29], using the linear axion model, the authors studied the optical conductivity with the phase transition between the normal phase and the superconducting phase.¹⁸ Thus, it would be instructive to compare the features in Fig. 3 and the result in [29]. To our knowledge, our work is the first holographic study considering the optical conductivity of (2.1) for the normal phase ($\Phi = 0$), i.e., the Gubser-Rocha model with the axion field.

We found one distinct feature between two holographic models at strong momentum relaxation region: unlike the linear axion model [29], at large k/μ , the Drude like peak in the normal phase does not disappear for the Gubser Rocha model (e.g., see dashed black (and red) line in Fig. 3(c)). In order to show this feature more clearly at strong momentum relaxation limit ($k/\mu \rightarrow \infty$), we take $\mu/k = 0$ and make the plot of the optical conductivity in Fig. 4(a).¹⁹

The non-vanishing Drude like peak in the strong momentum relaxation limit might be related to the fact that the Gubser-Rocha model produces linear- T resistivity unlike the linear axion model. For instance, at $\mu/k = 0$, both holographic models show the DC conductivity as

$$\sigma_{DC} = \sqrt{1 + \tilde{Q}} \left(1 + \frac{\mu^2}{k^2} \right) \sim \sqrt{1 + \tilde{Q}} \sim \frac{k}{2\sqrt{2}\pi T}, \quad (\text{Gubser-Rocha model}) \quad (3.10)$$

$$\sigma_{DC} = 1 + \frac{\mu^2}{k^2} \sim 1, \quad (\text{Linear axion model}) \quad (3.11)$$

¹⁸Although the linear axion model cannot exhibit the linear- T resistivity, it has been used to describe the metal/superconductor transition.

¹⁹One may directly compare Fig. 4(a) with Fig. 4(c) in [29].

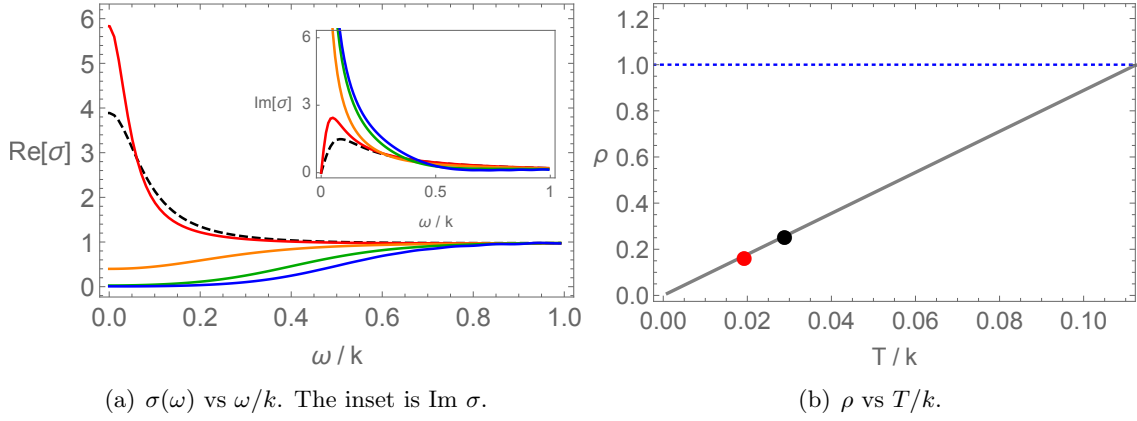


Figure 4. The electric conductivity at $\mu/k = 0$. **Left:** $\sigma(\omega)$ of the Gubser-Rocha model at $T/T_c = 1.5, 1, 0.93, 0.75, 0.41$ (dashed, red, orange, green, blue). **Right:** The DC resistivity ρ ($1/\sigma(\omega = 0)$) of two holographic models: the Gubser Rocha model (solid gray) (3.10), the linear axion model (dotted blue) (3.11). The black (red) dot corresponds to the DC limit of the black (red) line in Fig. 4(a): it shows that the numerical result of $\sigma(\omega = 0)$ is consistent with the analytic DC result.

where \tilde{Q} from the dilaton field plays an important role for the linear- T resistivity.²⁰

In Fig. 4(b), we display the DC conductivity of two holographic models: the Gubser Rocha model (solid gray) (3.10), the linear axion model (dotted blue) (3.11). The black (red) dot in Fig. 4(b) corresponds to the DC limit of the black (red) line in Fig. 4(a): it shows that the numerically computed $\sigma(\omega = 0)$ is consistent with the analytic DC result.²¹

Note that, at $\omega/k \rightarrow \infty$, $\sigma(\omega) = 1$ in both models. However, in the opposite limit, $\omega/k \rightarrow 0$, the linear axion model gives the constant value, i.e., $\sigma(\omega) = 1$ (3.11) unlike the Gubser-Rocha model (3.10). Thus, for the linear axion model, the optical conductivity of the normal phase would be a constant, $\sigma(\omega) = 1$, in all ω regime without producing a Drude like peak.

Two-fluid model and superfluid density: For superconducting phase (roughly $0.5 < T/T_c < 1$) in Fig. 3, $\text{Re}[\sigma]$ also has a remaining finite value at $\omega = 0$ in addition to the delta function by the Kramers-Kronig relation. This residual Drude-like peak may be interpreted by the two-fluid model [25] as a contribution from the normal component in the superconducting phase, which has also been observed in other holographic superconductor models such as linear-axion model [29], Q-lattice model [27], and Helical lattice model [24].

The two-fluid model demonstrates that the low frequency behavior of the optical conductivity can be fitted with the following formula:

$$\sigma(\omega) = i \frac{\rho_s}{\omega} + \frac{\rho_n \tau_r}{1 - i \omega \tau_r} + \rho_0, \quad (3.12)$$

²⁰(2.17) is used in (3.10) which corresponds to (2.15).

²¹Moreover, also note that the linear- T resistivity is robust above T_c (red dot) in Fig. 4(b), which is similar to experiments.

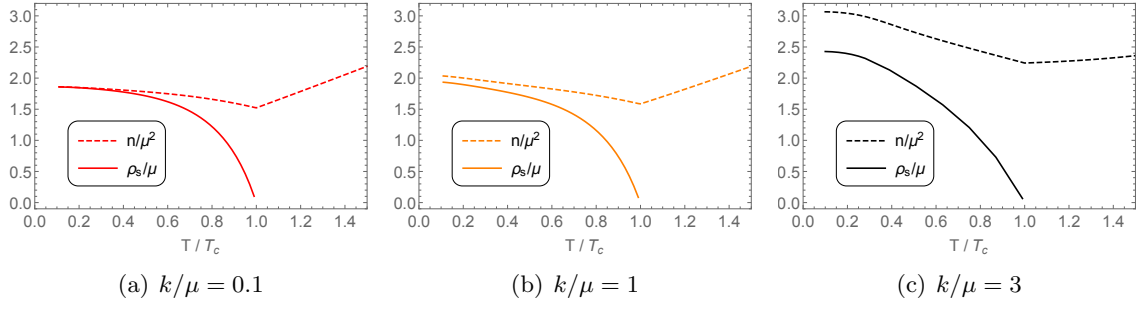


Figure 5. The charge density n , superfluid density ρ_s vs T/T_c . The gap between n and ρ_s at $T = 0$ opens at finite k/μ ($\tau = 1/\sqrt{3}$).

where ρ_s and ρ_n are defined as the superfluid density and the normal fluid density.²² τ_r is the relaxation time. ρ_0 may be related to the pair creation and can be used to fit the numerical data in the presence of the momentum relaxation [29].

The superfluid density ρ_s is our main interest to study Homes' law, which can be read off from the fitting curve (3.12). One interesting feature of ρ_s in holographic superconductors [24, 32, 33, 36] is that there is a finite gap at $T = 0$ between ρ_s and the charge density n in the presence of the momentum relaxation.²³ This also happens in our superconductor model. See Fig. 5. Thus, this non-vanishing gap at finite k/μ seems to be a generic feature of holographic superconductors.

We also find that, as T is lowered, ρ_0 and ρ_n are reduced while ρ_s is enhanced.²⁴ For the relaxation time τ_r , we find it is decreasing as T is lowered. The behavior of τ_r , at low T depends on holographic models: it is increasing in [25], it is decreasing first and then increasing in [27]. So, apparently, the more detailed analysis and the unified description for the relaxation time for holographic superconductor is still needed. We leave this subject as future work.

3.3 Homes' law at strong momentum relaxation

Now let us discuss Homes' law (1.1). Computing three quantities ($\rho_s(T = 0)$, T_c , $\sigma_{DC}(T_c)$) as a function of k/μ , we may check Homes' law at given τ .²⁵

Note that $\rho_s(T = 0)$ can be read off from (3.12) in principle. However, as one can see from Fig. 5, $\rho_s(T)$ does not reach to $T = 0$ due to the instability in our numerics. Thus, we extrapolate $\rho_s(T)$ up to zero temperature in order to obtain $\rho_s(T = 0)$. Other quantity for Homes' law, $\sigma_{DC}(T_c)$, is determined by (2.13) with a numerically computed T_c .

We first study Homes' law for the scaling case ($\tau = 1/\sqrt{3}$). In Fig. 6, we display ($\rho_s(T = 0)$, T_c , $\sigma_{DC}(T_c)$). As we increase k/μ , in the strong momentum relaxation regime,

²² ρ_s and ρ_n are supposed to be proportional to the superfluid density and the normal fluid density from the viewpoint of experiments or there could be prefactor $\pi/2$ in each terms. However, for the theoretical study of conductivity, we define the superfluid density and normal fluid density including all the factors.

²³The charge density n is defined by a subleading coefficient of A_t : $A_t = \mu - nz + \dots$ near AdS boundary. The normal fluid density would be given by the difference between n and ρ_s .

²⁴At small T , ρ_0 would be vanishing, however ρ_n could be finite even at $T = 0$ [25–27].

²⁵Recall that we have two parameters (τ , k/μ) in our setup.

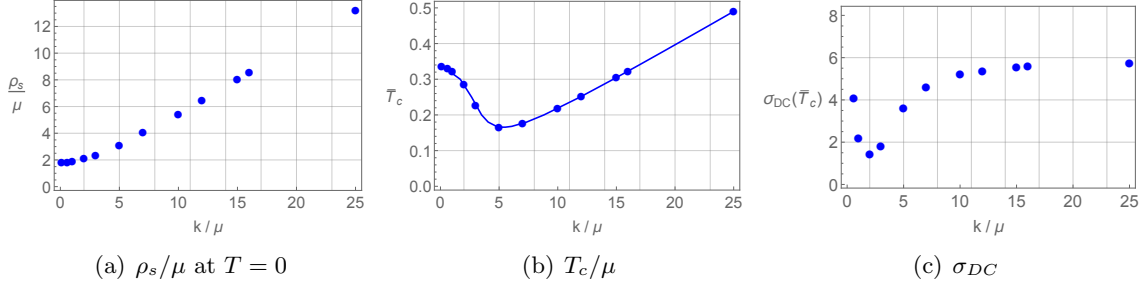


Figure 6. ρ_s, T_c , and $\sigma_{DC}(T_c)$ for $\tau = 1/\sqrt{3}$. \bar{T}_c is the shorthand notation for T_c/μ . The blue solid line corresponds to the one in Fig. 1.

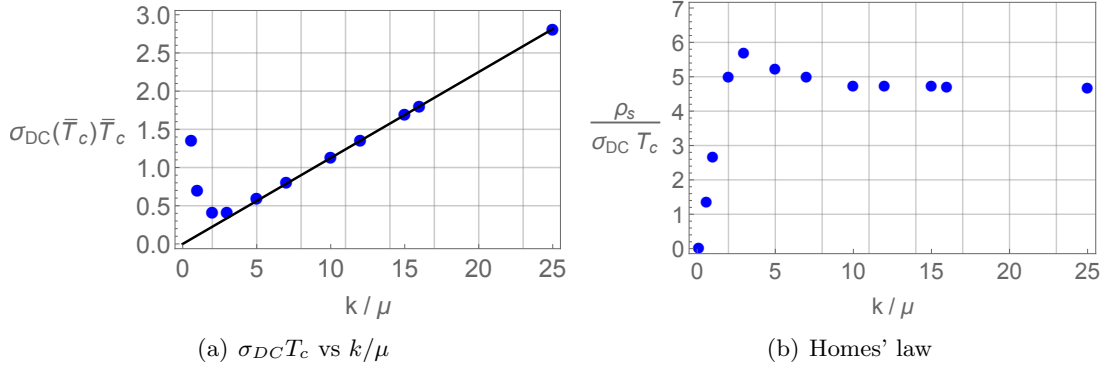


Figure 7. Left: $\sigma_{DC} T_c$ vs k . \bar{T}_c is the shorthand notation for T_c/μ . The black solid line is (3.13). **Right:** Checking Homes' law: Homes' law appears to hold in the strong momentum relaxation limit.

one can see that ρ_s and T_c are increasing linearly while σ_{DC} saturates to some constant.²⁶

Unlike the behavior of ρ_s and σ_{DC} , the increasing behavior of T_c is the distinct property not observed in other holographic studies, for instance, T_c tends to decrease or saturates to some value in [24, 32, 33].²⁷ Moreover, this increasing feature from T_c seems to play an important role for Homes' law as we show in shortly.

Homes' law with linear- T resistivity: Using the data in Fig. 6, we make a plot of the ratio $\rho_s/(\sigma_{DC} T_c)$ ($=: C$) as a function of k/μ in Fig. 7(b), and observe that the ratio C becomes a constant, $C \sim 4.7$, at $k/\mu \gg 1$ limit, i.e., Homes' law (1.1) appears to hold in the strong momentum relaxation limit. One may wonder if C remains a constant at $k/\mu > 25$ in Fig. 7(b). Evaluating C at $\mu/k = 0$, we confirmed that C is a constant around 4.7 in $k/\mu \gg 1$ limit.

Homes' law at strong momentum relaxation limit, the constant C , can be viewed as the cancelation of the two linearities in k/μ : one from ρ_s in Fig. 6(a) and the other from

²⁶ σ_{DC} tends to diverge in small k/μ region. This implies the infinite DC conductivity for the weak momentum relaxation.

²⁷In Fig. 6(b), the blue line corresponds to the one in Fig. 1. This implies that T_c obtained in the fully back-reacted background geometry is consistent with the one without the back-reaction.

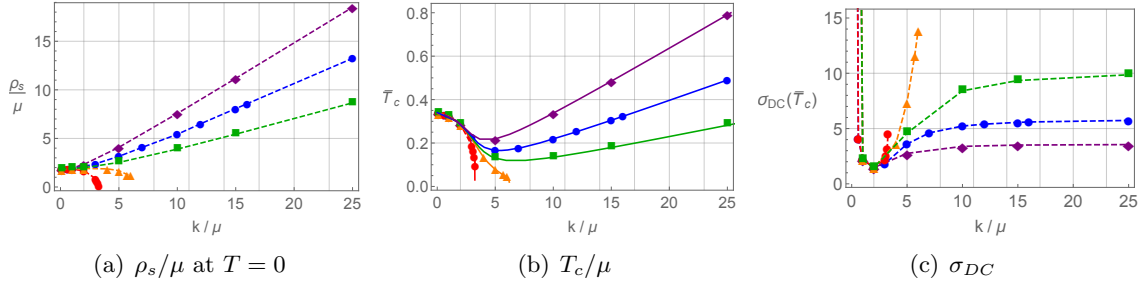


Figure 8. ρ_s/μ , T_c/μ , and σ_{DC} for $\tau = (0, \frac{1}{\sqrt{3}} \frac{8}{10}, \frac{1}{\sqrt{3}} \frac{9}{10}, \frac{1}{\sqrt{3}} \frac{10}{10}, \frac{1}{\sqrt{3}} \frac{12}{10})$ (red, orange, green, blue, purple). \bar{T}_c is the shorthand notation for T_c/μ . The solid lines in (b) are Fig. 1 and the dashed lines in (a), (c) are fitting curves.

$\sigma_{DC}T_c$ in Fig. 7(a). The linearity in Fig. 7(a), the black solid line, can be understood by

$$\sigma_{DC} \frac{T}{\mu} = \frac{1}{2\sqrt{2}\pi} \frac{k}{\mu}, \quad (3.13)$$

where the DC conductivity formula (2.15) is used. Note that linear- T resistivity in (2.15) plays a crucial role because (3.13) becomes T -independent so valid at $T \gtrsim T_c$. Alternatively, the linearity in Fig. 7(a) (or (3.13)) may be understood from the fact that T_c is linear in k (Fig. 6(b)) and σ_{DC} is constant (Fig. 6(c)).

3.4 The coupling τ dependence

Next, let us discuss the τ dependence in Homes' law.²⁸ We display the plots for $(\rho_s(T=0), T_c, \sigma_{DC}(T_c))$ with various τ in Fig. 8: blue dots in Fig. 8 correspond to Fig. 6 (i.e., the scaling case $\tau = 1/\sqrt{3}$).

ρ_s and T_c with τ : $\rho_s(T=0)$ in Fig. 8(a) shows the qualitatively similar behavior with T_c in Fig. 8(b): as we increase k/μ , at $\tau < \tau_c$ (red, orange), it is reduced while, at $\tau > \tau_c$ (green, blue, purple), it is linearly increasing.²⁹ One may understand the resemblance between $\rho_s(T=0)$ and T_c as follows. As can be seen in Fig. 5, $\rho_s(T)$ is zero at $T = T_c$ and monotonically increasing at $T < T_c$. Thus, in order to have a large (small) ρ_s at $T = 0$, T_c may need to be large (small) as well, i.e., $\rho_s(T=0) \sim T_c$.

Note that the solid lines in Fig. 8(b) are Fig. 1, i.e., T_c from the fully back-reacted geometry is consistent with the one without back-reaction. This may imply that ρ_s might also be understood in the probe limit. If one can develop the methodology to compute $\sigma(\omega)$ only with the IR geometry (the $T = 0$ analysis), we suspect that the numerical result in Fig. 8(a) might also be confirmed in a simple probe limit with the scaling property (2.21).

²⁸In this paper, we perform the computation up to $\tau = \frac{1}{\sqrt{3}} \frac{12}{10}$ because of the stability in our numerics, which might be enough to discuss Homes' law.

²⁹This would be another universal relation similar to Homes' law, called Uemura's law which holds only for underdoped cuprates [7, 8]: $\rho_s(T=0) = \tilde{C}T_c$ with a universal constant \tilde{C} .

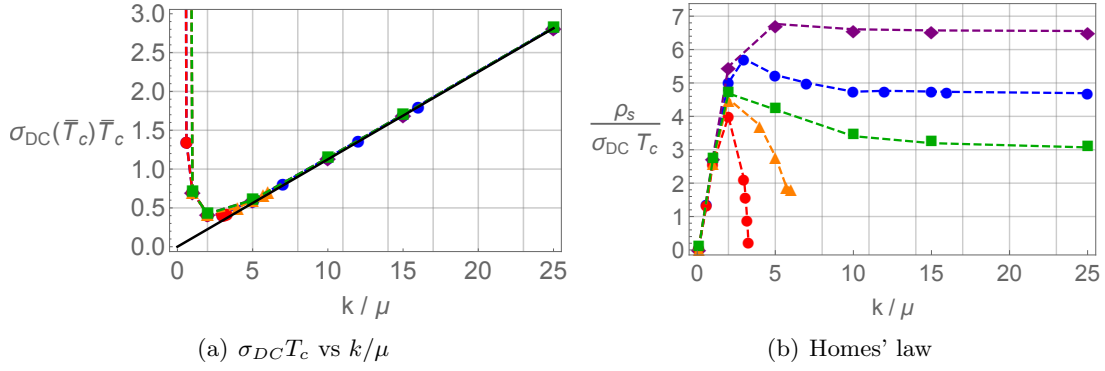


Figure 9. **Left:** $\sigma_{DC}T_c$ vs k . The black solid line is (3.13). **Right:** Checking Homes' law with $\tau = (0, \frac{1}{\sqrt{3}}\frac{8}{10}, \frac{1}{\sqrt{3}}\frac{9}{10}, \frac{1}{\sqrt{3}}\frac{10}{10}, \frac{1}{\sqrt{3}}\frac{12}{10})$ (red, orange, green, blue, purple).

$\sigma_{DC}(T_c)$ **with** τ : In Fig. 8(c), unlike ρ_s , there is no resemblance between $\sigma_{DC}(T_c)$ and T_c . At small k/μ , σ_{DC} is diverging independent of τ , which reflects the fact the conductivity is infinite at zero momentum relaxation.

On the other hand, at larger k/μ , one can see the τ dependence on $\sigma_{DC}(T_c)$. At $\tau < \tau_c$ (red, orange), it is increasing while, at $\tau > \tau_c$ (green, blue, purple), it saturates to some constant. Note that the behavior of $\sigma_{DC}(T_c)$ at large k/μ depends on the holographic models: for instance, it is increasing in the Q-lattice model [33] or saturated in the linear axion model [32].

Homes' law at $\tau > \tau_c$: With the data in Fig. 8, we find Homes' law (1.1) at the strong momentum relaxation limit for $\tau > \tau_c$ (green, blue, purple): i.e., C become a constant at $k/\mu \gg 1$. See Fig. 9(b). As did in the scaling case ($\tau = 1/\sqrt{3}$) in Fig. 7(a), Homes' law at $\tau > \tau_c$ can be understood from the cancelation of the two linearities in k/μ : one from ρ_s (Fig. 8(a)) and the other from the linear- T resistivity (Fig. 9(a)).

We also find that the saturating value of C depends on the value of τ . Thus, τ might be used to match the experiment data: $C = 4.4$ for ab-plane high T_c superconductors as well as clean BCS superconductors and $C = 8.1$ for c-axis high T_c superconductor and BCS superconductors in the dirty limit.

4 Conclusions

We have investigated Homes' law (1.1) by computing the critical temperature T_c , the superfluid density ρ_s at zero temperature, and the DC conductivity σ_{DC} at T_c in a holographic superconductor based on the Gubser-Rocha model (2.1) with the minimally chosen coupling term $B(\phi)$:

$$B(\phi) = M^2 \cosh(\tau\phi) , \quad (4.1)$$

where it corresponds to the mass term of the complex scalar field, M^2 , at $\tau = 0$. The action (2.1) also contains the axion field to study the momentum relaxation where its strength is

denoted as k/μ . In this setup, Homes' law means that $C := \rho_s/(\sigma_{DC}T_c)$ is independent of the momentum relaxation.

The Gubser-Rocha model, a *normal* phase, is appealing in that the linear- T resistivity can be obtained at strong momentum relaxation limit ($k/\mu \gg 1$) above T_c . Considering the complex scalar field with the Gubser-Rocha model, we find that, in order to study the *superconducting* phase at $k/\mu \gg 1$, τ in the coupling (4.1) is important. We show that the conditions to study a holographic superconductor having the linear- T resistivity above T_c would be:

$$\text{i) } \tau > \tau_c; \quad \text{ii) } k/\mu \gg 1, \quad (4.2)$$

where $\tau_c \neq 0$ can be determined numerically from the instability analysis for T_c . The first condition i) in (4.2) means that if τ is smaller than τ_c the superconducting phase does not exist at large k/μ . In particular, the trivial coupling term $B(\phi) = M^2$ ($\tau = 0$ case), the mass term of the complex scalar field, used in previous literature can not capture a complete feature of the superconducting phase at $k/\mu \gg 1$.

With the condition (4.2), we find Homes' law can hold in the strong momentum relaxation limit, i.e., C becomes a constant at $k/\mu \gg 1$ limit. In [48], it is argued that if the momentum is relaxed *quickly(strongly)*, which is an extrinsic so non-universal effect, transport can be governed by an intrinsic and universal effect such as diffusion of energy and charge. Thus, the universality of linear- T resistivity may appear in the regime of *strong* momentum relaxation (so called the *incoherent* regime). Consequently, Homes' law can appear also in the strong momentum relaxation limit.

Furthermore, we showed that Homes' law at $k/\mu \gg 1$ can be understood from the cancelation of the two linearities in k/μ : one from $\rho_s(T = 0)$ (numerical result) and the other from the linear- T resistivity (analytic result) (3.13). It will be interesting to show the linearity of $\rho_s(T = 0)$ in k/μ also analytically. If one can develop the method to compute the optical conductivity with the IR geometry ($T = 0$ analysis) in the superconducting phase³⁰, we suspect that the linearity of $\rho_s(T = 0)$ in k/μ might be related with the IR scaling property of the coupling $B(\phi)$ (2.21).

We find that the value of C at $k/\mu \gg 1$ depends on the value of τ so τ can be used to match the experiment data: $C = 4.4$ for ab-plane high T_c superconductors as well as clean BCS superconductors and $C = 8.1$ for c-axis high T_c superconductor and BCS superconductors in the dirty limit.

It may also be interesting to study Homes' law with the holographic models having other IR geometries [55, 56, 61] together with linear T resistivity. In [56], authors found that when the IR geometry is governed by a finite dynamical exponent z and a hyperscaling violating exponent θ unlike the Gubser-Rocha model ($z \rightarrow \infty, \theta \rightarrow -\infty$), the linear- T resistivity can also exhibit at high temperature if the momentum relaxation is strong. Therefore, one may investigate how much general our results in this paper are. One may also check if $\tau > \tau_c$ condition in (4.2) is necessary for Homes' law in more generic setup. We leave these subjects as future work and hope to address them in the near future.

³⁰In [58–60], the analytic IR geometry is given for $M^2 = 0, \tau = 0$ and $k/\mu = 0$.

Acknowledgments

We would like to thank Yongjun Ahn for valuable discussions and correspondence. This work was supported by the National Key R&D Program of China (Grant No. 2018FYA0305800), Project 12035016 supported by National Natural Science Foundation of China, the Strategic Priority Research Program of Chinese Academy of Sciences, Grant No. XDB28000000, Basic Science Research Program through the National Research Foundation of Korea (NRF) funded by the Ministry of Science, ICT & Future Planning (NRF- 2021R1A2C1006791) and GIST Research Institute(GRI) grant funded by the GIST in 2021.

References

- [1] S. A. Hartnoll, A. Lucas and S. Sachdev, *Holographic quantum matter*, [1612.07324](#).
- [2] J. Zaanen, Y.-W. Sun, Y. Liu and K. Schalm, *Holographic Duality in Condensed Matter Physics*. Cambridge Univ. Press, 2015.
- [3] M. Ammon and J. Erdmenger, *Gauge/gravity duality*. Cambridge Univ. Pr., Cambridge, UK, 2015.
- [4] M. Baggioli, *Applied Holography: A Practical Mini-Course*. SpringerBriefs in Physics. Springer, 2019, [10.1007/978-3-030-35184-7](#).
- [5] S. A. Hartnoll, *Lectures on holographic methods for condensed matter physics*, *Class.Quant.Grav.* **26** (2009) 224002, [[0903.3246](#)].
- [6] C. P. Herzog, *Lectures on Holographic Superfluidity and Superconductivity*, *J.Phys.A* **A42** (2009) 343001, [[0904.1975](#)].
- [7] C. C. Homes, S. V. Dordevic, T. Valla and M. Strongin, *Scaling of the superfluid density in high-temperature superconductors*, *Phys. Rev. B* **72**, **134517** (2005) (8, [[cond-mat/0410719](#)]).
- [8] C. Homes, S. Dordevic, M. Strongin, D. Bonn, R. Liang et al., *Universal scaling relation in high-temperature superconductors*, *Nature* **430** (2004) 539, [[cond-mat/0404216](#)].
- [9] S. A. Hartnoll, C. P. Herzog and G. T. Horowitz, *Building a Holographic Superconductor*, *Phys.Rev.Lett.* **101** (2008) 031601, [[0803.3295](#)].
- [10] S. A. Hartnoll, C. P. Herzog and G. T. Horowitz, *Holographic Superconductors*, *JHEP* **0812** (2008) 015, [[0810.1563](#)].
- [11] G. T. Horowitz, *Introduction to Holographic Superconductors*, [1002.1722](#).
- [12] R.-G. Cai, L. Li, L.-F. Li and R.-Q. Yang, *Introduction to Holographic Superconductor Models*, *Sci. China Phys. Mech. Astron.* **58** (2015) 060401, [[1502.00437](#)].
- [13] K. Y. Kim and M. Taylor, *Holographic d-wave superconductors*, *JHEP* **08** (2013) 112, [[1304.6729](#)].
- [14] B. Gout  raux and E. Mefford, *Normal charge densities in quantum critical superfluids*, *Phys. Rev. Lett.* **124** (2020) 161604, [[1912.08849](#)].
- [15] B. Gout  raux and E. Mefford, *Non-vanishing zero-temperature normal density in holographic superfluids*, *JHEP* **11** (2020) 091, [[2008.02289](#)].
- [16] D. Arean, M. Baggioli, S. Grieninger and K. Landsteiner, *A Holographic Superfluid Symphony*, [2107.08802](#).

- [17] A. Donos, P. Kailidis and C. Pantelidou, *Dissipation in holographic superfluids*, *JHEP* **09** (2021) 134, [[2107.03680](#)].
- [18] M. Ammon, D. Arean, M. Baggioli, S. Gray and S. Griener, *Pseudo-spontaneous $U(1)$ Symmetry Breaking in Hydrodynamics and Holography*, [2111.10305](#).
- [19] G. T. Horowitz, J. E. Santos and D. Tong, *Optical Conductivity with Holographic Lattices*, *JHEP* **1207** (2012) 168, [[1204.0519](#)].
- [20] D. Vegh, *Holography without translational symmetry*, [1301.0537](#).
- [21] A. Donos and J. P. Gauntlett, *Holographic Q -lattices*, *JHEP* **1404** (2014) 040, [[1311.3292](#)].
- [22] T. Andrade and B. Withers, *A simple holographic model of momentum relaxation*, *JHEP* **1405** (2014) 101, [[1311.5157](#)].
- [23] A. Donos and S. A. Hartnoll, *Interaction-driven localization in holography*, *Nature Phys.* **9** (2013) 649–655, [[1212.2998](#)].
- [24] J. Erdmenger, B. Herwerth, S. Klug, R. Meyer and K. Schalm, *S-Wave Superconductivity in Anisotropic Holographic Insulators*, *JHEP* **05** (2015) 094, [[1501.07615](#)].
- [25] G. T. Horowitz and J. E. Santos, *General Relativity and the Cuprates*, [1302.6586](#).
- [26] H. B. Zeng and J.-P. Wu, *Holographic superconductors from the massive gravity*, *Phys.Rev.* **D90** (2014) 046001, [[1404.5321](#)].
- [27] Y. Ling, P. Liu, C. Niu, J.-P. Wu and Z.-Y. Xian, *Holographic Superconductor on Q -lattice*, *JHEP* **02** (2015) 059, [[1410.6761](#)].
- [28] T. Andrade and S. A. Gentle, *Relaxed superconductors*, [1412.6521](#).
- [29] K.-Y. Kim, K. K. Kim and M. Park, *A Simple Holographic Superconductor with Momentum Relaxation*, *JHEP* **04** (2015) 152, [[1501.00446](#)].
- [30] M. Baggioli and M. Goykhman, *Phases of holographic superconductors with broken translational symmetry*, *JHEP* **07** (2015) 035, [[1504.05561](#)].
- [31] M. Baggioli and M. Goykhman, *Under The Dome: Doped holographic superconductors with broken translational symmetry*, *JHEP* **01** (2016) 011, [[1510.06363](#)].
- [32] K. K. Kim, M. Park and K.-Y. Kim, *Ward identity and Homes' law in a holographic superconductor with momentum relaxation*, *JHEP* **10** (2016) 041, [[1604.06205](#)].
- [33] K.-Y. Kim and C. Niu, *Homes' law in Holographic Superconductor with Q -lattices*, *JHEP* **10** (2016) 144, [[1608.04653](#)].
- [34] Y. Ling and X. Zheng, *Holographic superconductor with momentum relaxation and Weyl correction*, *Nucl. Phys.* **B917** (2017) 1–18, [[1609.09717](#)].
- [35] H.-S. Jeong, K.-Y. Kim and C. Niu, *Linear- T resistivity at high temperature*, *JHEP* **10** (2018) 191, [[1806.07739](#)].
- [36] J. Erdmenger, P. Kerner and S. Muller, *Towards a Holographic Realization of Homes' Law*, *JHEP* **1210** (2012) 021, [[1206.5305](#)].
- [37] K.-Y. Kim, K. K. Kim, Y. Seo and S.-J. Sin, *Coherent/incoherent metal transition in a holographic model*, *JHEP* **12** (2014) 170, [[1409.8346](#)].
- [38] K.-Y. Kim, K. K. Kim, Y. Seo and S.-J. Sin, *Gauge Invariance and Holographic Renormalization*, *Phys. Lett.* **B749** (2015) 108–114, [[1502.02100](#)].

- [39] K.-Y. Kim, K. K. Kim, Y. Seo and S.-J. Sin, *Thermoelectric Conductivities at Finite Magnetic Field and the Nernst Effect*, *JHEP* **07** (2015) 027, [[1502.05386](#)].
- [40] H.-S. Jeong, K.-Y. Kim, Y. Seo, S.-J. Sin and S.-Y. Wu, *Holographic Spectral Functions with Momentum Relaxation*, *Phys. Rev. D* **102** (2020) 026017, [[1910.11034](#)].
- [41] M. Baggioli, K.-Y. Kim, L. Li and W.-J. Li, *Holographic Axion Model: a simple gravitational tool for quantum matter*, *Sci. China Phys. Mech. Astron.* **64** (2021) 270001, [[2101.01892](#)].
- [42] S. S. Gubser and F. D. Rocha, *Peculiar properties of a charged dilatonic black hole in AdS_5* , *Phys.Rev.* **D81** (2010) 046001, [[0911.2898](#)].
- [43] R. A. Davison, K. Schalm and J. Zaanen, *Holographic duality and the resistivity of strange metals*, *Phys. Rev.* **B89** (2014) 245116, [[1311.2451](#)].
- [44] Z. Zhou, Y. Ling and J.-P. Wu, *Holographic incoherent transport in Einstein-Maxwell-dilaton Gravity*, *Phys. Rev.* **D94** (2016) 106015, [[1512.01434](#)].
- [45] K.-Y. Kim and C. Niu, *Diffusion and Butterfly Velocity at Finite Density*, *JHEP* **06** (2017) 030, [[1704.00947](#)].
- [46] Y. Liu and X.-M. Wu, *Breakdown of hydrodynamics from holographic pole collision*, [2111.07770](#).
- [47] J. Zaanen, *Superconductivity: Why the temperature is high*, *Nature* **430** (07, 2004) 512–513.
- [48] S. A. Hartnoll, *Theory of universal incoherent metallic transport*, *Nature Phys.* **11** (2015) 54, [[1405.3651](#)].
- [49] A. Lucas, S. Sachdev and K. Schalm, *Scale-invariant hyperscaling-violating holographic theories and the resistivity of strange metals with random-field disorder*, *Phys. Rev. D* **89** (2014) 066018, [[1401.7993](#)].
- [50] S. Cremonini and L. Li, *Criteria For Superfluid Instabilities of Geometries with Hyperscaling Violation*, *JHEP* **11** (2016) 137, [[1606.02745](#)].
- [51] R. A. Davison, *Momentum relaxation in holographic massive gravity*, *Phys.Rev.* **D88** (2013) 086003, [[1306.5792](#)].
- [52] M. Blake and D. Tong, *Universal Resistivity from Holographic Massive Gravity*, *Phys.Rev.* **D88** (2013) 106004, [[1308.4970](#)].
- [53] M. Blake, D. Tong and D. Vegh, *Holographic Lattices Give the Graviton a Mass*, *Phys.Rev.Lett.* **112** (2014) 071602, [[1310.3832](#)].
- [54] A. Donos and J. P. Gauntlett, *Thermoelectric DC conductivities from black hole horizons*, *JHEP* **11** (2014) 081, [[1406.4742](#)].
- [55] B. Goutéraux, *Charge transport in holography with momentum dissipation*, *JHEP* **1404** (2014) 181, [[1401.5436](#)].
- [56] Y. Ahn, H.-S. Jeong, D. Ahn and K.-Y. Kim, *Linear- T resistivity from low to high temperature: axion-dilaton theories*, *JHEP* **04** (2020) 153, [[1907.12168](#)].
- [57] Y. Ling, C. Niu, J.-P. Wu and Z.-Y. Xian, *Holographic Lattice in Einstein-Maxwell-Dilaton Gravity*, *JHEP* **1311** (2013) 006, [[1309.4580](#)].
- [58] G. T. Horowitz and M. M. Roberts, *Zero Temperature Limit of Holographic Superconductors*, *JHEP* **0911** (2009) 015, [[0908.3677](#)].
- [59] P. Basu, *Low temperature properties of holographic condensates*, *JHEP* **03** (2011) 142,

[[1101.0215](#)].

- [60] R.-Q. Yang, H.-S. Jeong, C. Niu and K.-Y. Kim, *Complexity of Holographic Superconductors*, *JHEP* **04** (2019) 146, [[1902.07586](#)].
- [61] H.-S. Jeong, Y. Ahn, D. Ahn, C. Niu, W.-J. Li and K.-Y. Kim, *Thermal diffusivity and butterfly velocity in anisotropic Q-Lattice models*, *JHEP* **01** (2018) 140, [[1708.08822](#)].